



# Polyethylenimine and sodium cholate-modified ethosomes complex as multidrug carrier for the treatment of melanoma through transdermal delivery

Linlin Ma<sup>‡,1</sup>, Xiaoyun Wang<sup>‡,4</sup>, Jinglei Wu<sup>‡,1</sup>, Dongdong Zhang<sup>1</sup>, Lin Zhang<sup>2,3</sup>, Xinran Song<sup>1</sup>, Huoyan Hong<sup>1</sup>, Chuanglong He<sup>1</sup>, Xiumei Mo<sup>1</sup>, Sufang Wu<sup>\*\*\*,4</sup>, Guoyin Kai<sup>\*\*2</sup> & Hongsheng Wang<sup>\*,1</sup>

<sup>1</sup>Key Laboratory of Science & Technology of Eco-Textile, Ministry of Education, College of Chemistry, Chemical Engineering & Biotechnology, Donghua University, Shanghai 201620, PR China

<sup>2</sup>Laboratory of Medicinal Plant Biotechnology, College of Pharmaceutical Sciences, Zhejiang Chinese Medical University, Hangzhou, 311402, PR China

<sup>3</sup>Department of Pharmacy, Shaoxing People's Hospital, Shaoxing Hospital of Zhejiang University, Shaoxing 31200, PR China

<sup>4</sup>Department of Obstetrics & Gynecology, Shanghai First People's Hospital Affiliated to Shanghai Jiaotong University, Shanghai, 201620, PR China

\*Author for correspondence: Tel.: +86 21 6779 2742; Fax: +86 21 6779 2742; [wsh@dhu.edu.cn](mailto:wsh@dhu.edu.cn)

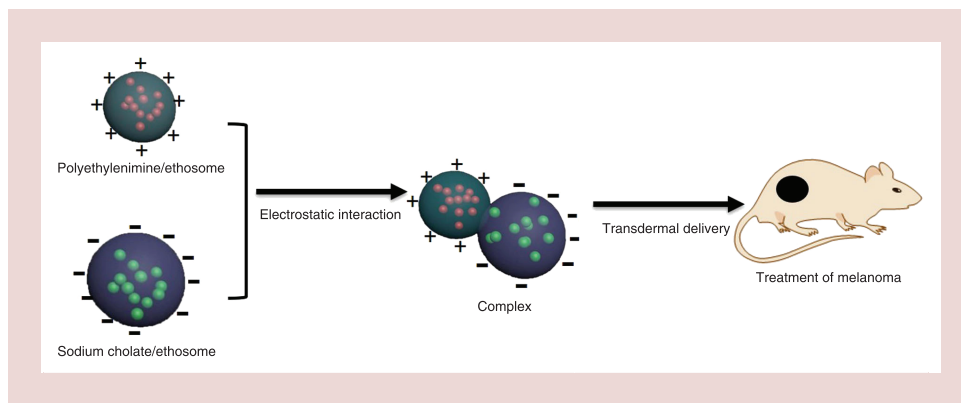
\*\*Author for correspondence: [kaiguoyin@163.com](mailto:kaiguoyin@163.com)

\*\*\*Author for correspondence: [wsf\\_sfph@sjtu.edu.cn](mailto:wsf_sfph@sjtu.edu.cn)

‡ Authors contributed equally

**Aim:** Multidrug resistance is the main reason for the failure of chemotherapy during the treatment of the tumor. To overcome multidrug resistance, this study attempts to develop a novel transdermal drug-delivery system (TDDS) loading cytotoxic drug and chemosensitizer. **Materials & methods:** The polyethylenimine-modified ethosomes (Eth<sup>-PEI</sup>) and sodium cholate-modified ethosomes (Eth<sup>-SC</sup>) were firstly fabricated, and then a novel TDDS based on the carriers complex of Eth<sup>-PEI</sup>/Eth<sup>-SC</sup> was prepared by electrostatic interaction and evaluated both *in vitro* and *in vivo*. **Results:** The Eth<sup>-PEI</sup>/Eth<sup>-SC</sup> showed the excellent antitumor effect on treating melanoma, using doxorubicin and curcumin as the cytotoxic drug and chemosensitizer, respectively. **Conclusion:** The as-prepared TDDS composed of Eth<sup>-PEI</sup>/Eth<sup>-SC</sup> loading multidrug is an effective means for treating melanoma.

## Graphical abstract:



First draft submitted: 18 October 2018; Accepted for publication: 1 July 2019; Published online: 28 August 2019

**Keywords:** anticancer • curcumin • doxorubicin • ethosome • melanoma • transdermal drug delivery

Chemotherapy is one of the main effective methods for long-term cancer cure [1–3]. However, drug resistance is almost unavoidable during the chemotherapy of tumor with single-agent drug, and multidrug resistance (MDR) is the main reason for the failure of chemotherapy [4]. The combination of cytotoxic agent and chemosensitizer has been thought effective to overcome MDR and reduce side effects by modulating multiple signaling pathways in cancer cells [4–6]. Though doxorubicin (DOX) is frequently used for the treatment of cancer, the use of free DOX is also rather hampered due to MDR as well as cardiotoxicity and nephrotoxicity in clinical trials [7–9]. The main molecular mechanisms of primary or secondary drug resistance to DOX was reported to be the overexpression of P-glycoprotein encoded by *MDR1* [8]. Curcumin (CUR), a polyphenol from the *Curcuma longa* L., can act as a chemosensitizer co-administered with various efficacious anticancer agents and has been proved no toxic side effects even at high doses [10–13]. Recently, several studies have demonstrated the synergistic effects of CUR and DOX, which triumphantly enhanced the treatment efficacy of some cancers [14–18].

Another optimum solution for MDR is choosing a carrier which can wrap and transport cytotoxic drugs into tumor site directly [4]. Doxil and Caelyx, the formulations of DOX encapsulated inside liposomes, had been approved for the adjuvant therapy by US FDA in 1995 [19]. A liposome is a kind of nanoparticle with a cell membrane-like structure which can easily fuse with the cell membrane, and has become a well-established carrier in tumor treatment [20,21]. To best satisfy the therapeutic demands, the development of liposomes put emphasis on surface modification [22]. Among them, cationic liposomes achieved cellular delivery of drugs efficiently due to its surface positive charge and high deformability [23]. However, high positive charges of cationic liposomes can also lead to severe toxicity in normal host cells, and occasionally cause a hypersensitivity reaction [24]. Therefore, it is critical to balance between a high transfection efficiency and low cytotoxicity of the liposomes.

An ethosome is a modified form of liposome that contains a relatively low concentration of ethanol [23]. In recent years, ethosome has been intensively studied as a drug carrier applied in transdermal drug delivery system (TDDS) for its high transdermal efficiency and stability [25]. TDDS can transport drugs into the systemic blood without the shortcomings of the hepatic first-pass effect and potential infection, compared with traditional drug administrations (usually intravenous and oral) [26,27]. TDDS has also been reported to have unique advantages in improving the control and treatment of superficial cancers, enhancing the efficiency of drug administration to the lymphatic system and inducing an immune response (transcutaneous immunization) through antigen presenting cells [28].

Based on the above knowledge, we hypothesized that a TDDS with both cationic and anionic ethosomes loading cytotoxic drug and chemosensitizer, respectively could achieve the desired effect on the treatment of cancers, especially for those occurred in the superficial tissues such as cutaneous melanoma. Here, a novel TDDS based on the ethosomes complex including polyethyleneimine (PEI)-modified ethosomes (Eth<sup>PEI</sup>) and sodium cholate (SC)-modified ethosomes (Eth<sup>SC</sup>; the two kinds of carriers would load different drugs, typically cytotoxic drug and chemosensitizer, respectively) were generated through electrostatic interaction. The carriers complex with different amount ratio of Eth<sup>PEI</sup> and Eth<sup>SC</sup> were prepared and characterized. The cell uptake and transdermal performance of the carriers complex were assessed *in vitro* using fluorescent agents. Furthermore, with the DOX and CUR as model drugs (CUR@Eth<sup>PEI</sup>/DOX@Eth<sup>SC</sup>), the therapeutic effect on melanoma of this TDDS was examined both *in vitro* and *in vivo*.

## Materials & Methods

### Materials

Fluorescein isothiocyanate (FITC), phosphatidyl choline (SC), 3-(4,5-dimethyl-2-thiazolyl)-2,5-diphenyl-2-H-tetrazolium bromidecholesterol (MTT), octadecylamine and PEI (Mw = 25 kDa) were purchased from Sigma-Aldrich (Shanghai, China). SC was purchased from Beijing Lark Technology Co. Ltd (Beijing, China). Rhodamine B (RB) was purchased from Sangon Biological Engineering Co. Ltd (Shanghai, China). Ultrapure water was used throughout this study. B16 cell line was provided by the Institute of Biochemistry and Cell Biology Sciences, Chinese Academy of Sciences (Shanghai, China). SD rats and C57BL/6 mice were purchased from Shanghai SLAC Laboratory Animal Co. Ltd (Shanghai, China).

### Preparation & characterization of the modified ethosomes

Ethosome was synthesized according to the thin layer evaporation technique [29]. Briefly, 100 mg lecithin and 10 mg cholesterol were sufficiently dissolved in 5 ml ethanol, and then the solution was evaporated by the vacuum

rotary evaporation to obtain the dry film. After that, the formed thin film was dissolved in 10 ml of H<sub>2</sub>O/ethanol (8:2 in volume), and 5 mg of PEI or SC was added into the solution and fully stirred for 30 min. Subsequently, Eth<sup>-PEI</sup> or Eth<sup>-SC</sup> was uniformly dispersed in solution after ultrasonic broken. The carriers complex was obtained by mixing the Eth<sup>-PEI</sup> solution with Eth<sup>-SC</sup> and incubated for 1 h at room temperature. The volume ratio of Eth<sup>-PEI</sup> to Eth<sup>-SC</sup> in the complex is ranging from 9:1, 8:2, 7:3, 6:4 to 5:5, which were denoted as Eth<sup>-PEI</sup>/Eth<sup>-SC</sup>(9:1), Eth<sup>-PEI</sup>/Eth<sup>-SC</sup>(8:2), Eth<sup>-PEI</sup>/Eth<sup>-SC</sup>(7:3), Eth<sup>-PEI</sup>/Eth<sup>-SC</sup>(6:4), Eth<sup>-PEI</sup>/Eth<sup>-SC</sup>(5:5), respectively. In the above process, the different drug-loaded Eth<sup>-PEI</sup> or Eth<sup>-SC</sup>(RB@Eth<sup>-PEI</sup>, FITC@Eth<sup>-SC</sup>, CUR@Eth<sup>-PEI</sup>, DOX@Eth<sup>-SC</sup>) can be obtained by replacing the H<sub>2</sub>O/ethanol (8:2 in volume) with different drugs solution (H<sub>2</sub>O/ethanol, 8:2 in volume). Mixing 7 ml of RB@Eth<sup>-PEI</sup> or CUR@Eth<sup>-PEI</sup> with 3 ml FITC@Eth<sup>-SC</sup> or DOX@Eth<sup>-SC</sup> to get the complex of RB@Eth<sup>-PEI</sup>/FITC@Eth<sup>-SC</sup>(7:3) or CUR@Eth<sup>-PEI</sup>/DOX@Eth<sup>-SC</sup>(7:3).

The attenuated total reflection–Fourier transform infrared spectroscopy (ATR-FTIR) of the modified ethosomes was scanned from 400 to 4000 cm<sup>-1</sup> using an ATR-FTIR spectrometer (Nicolet 6700, Thermo Fisher Scientific, WI, USA). 1 ml of uniform ethosomes solution was transferred to the ζ-potential sample pool and the colorimetric dish to measure the ζ-potential and particle size using Zetasizer Nano ZS instrument (Malvern, UK) [30]. The morphology of the ethosomes was examined by transmission electron microscopy (TEM; JEM-2100F, Jeol, Tokyo, Japan).

### Cellular uptake assay of the carriers complex

The cytophagic performance of the ethosomes was detected by B16 cells uptake assay using RB and FITC as model drugs *in vitro*. A certain amount of RB or FITC was added to the thin film mixed with PEI or SC solution according to the above-mentioned method and then RB@Eth<sup>-PEI</sup> and FITC@Eth<sup>-SC</sup> were gained. A total of 7 ml of RB@Eth<sup>-PEI</sup> was mixed with 3 ml FITC@Eth<sup>-SC</sup> to get the complex of RB@Eth<sup>-PEI</sup>/FITC@Eth<sup>-SC</sup>(7:3). The free RB and FITC dispersed in 10 ml of H<sub>2</sub>O/ethanol (8:2 in volume) were prepared as a control. All of the obtained samples were stored at 4°C for further use. B16 cells were directly seeded into 96-wells at the same density of  $2 \times 10^4$  cells/well. After being cultured for 24 h, the cell medium was replaced with 100 μl fresh DMEM (serum-free) and incubated for 2 h, then the medium was taken out and the cells were rinsed for three-times using phosphate-buffered saline (PBS). At last, the cells were imaged with fluorescence microscopy. The fluorescence intensity was calculated out by semi-quantitative analysis using software (Image J) and the number of the cells ingested model drugs (RB or FITC) was also evaluated by the semi-quantitative analysis of the fluorescence images using 1600–2000 cells on per area.

### *In vitro* transdermal performance of the carriers complex

The transdermal performance of the modified ethosomes was examined by Franz vertical diffusion method with RB and FITC as the model drugs. In order to imitate the physiological environment of the human body, PBS buffer was used as receiving liquid and temperature was set to 37°C according to the previous studies [31,32]. The abdominal hair of SD rat (female, weighing approximately 180 g) was shaved and the skin was excised carefully from abdomen after the mice were sacrificed with diethyl ether. The intact skin was placed on the receiving pool (the dermis tightly contacted with PBS buffer). A total of 2 ml of receiving solution was obtained and supplemented with the same volume of fresh PBS every 2 h. After 48 h, the skin was dehydrated, paraffin-embedded and sequentially sectioned. Fluorescence distribution in the skin was observed using fluorescence microscopy. All samples collected from the receiving solution were detected by a microplate reader (Multiskan MK3, Thermo Fisher Scientific) at 492 nm.

### *In vitro* antitumor test of the multidrug-loaded carriers complex

MTT assay was performed to evaluate the anticancer effect of drug-loaded ethosomes (CUR and DOX were loaded into Eth<sup>-PEI</sup> and Eth<sup>-SC</sup>, respectively). B16 cells were incubated 24 h at an initial density of  $2 \times 10^4$  cells/well in 96-wells plate. Then, the cells were treated with empty or drug-loaded ethosomes (Table 1) for 12 or 24 h. The concentration of DOX and CUR was set as 3 and 7 μg/ml, respectively according to the previous study [17]. At the time point, every well was rinsed three-times using PBS solution and then added with 100 μl fresh DMEM medium containing 10% MTT solution. After incubated for 4 h at 37°C, the medium was replaced with the same volume of dimethyl sulfoxide and shaken for 30 min in table oscillator. And then, the absorption of each well at 492 nm was measured with a microplate reader (Multiskan MK3, Thermo Fisher Scientific) and the background value of cell unseeded samples was taken out correspondingly.

Table 1. The *in vitro* tested groups and their additives.

	Cell medium	Eth <sup>PEI</sup>	Eth <sup>SC</sup>	CUR@Eth <sup>PEI</sup>	DOX@Eth <sup>SC</sup>
Control	1000 $\mu$ l	–	–	–	–
Eth <sup>PEI</sup>	995 $\mu$ l	5 $\mu$ l	–	–	–
Eth <sup>SC</sup>	995 $\mu$ l	–	5 $\mu$ l	–	–
Eth <sup>PEI</sup> / Eth <sup>SC</sup> (7:3)	995 $\mu$ l	3.5 $\mu$ l	1.5 $\mu$ l	–	–
CUR@Eth <sup>PEI</sup>	995 $\mu$ l	1.5 $\mu$ l	–	3.5 $\mu$ l	–
DOX@Eth <sup>SC</sup>	995 $\mu$ l	–	3.5 $\mu$ l	–	1.5 $\mu$ l
CUR@Eth <sup>PEI</sup> / DOX@Eth <sup>SC</sup> (7:3)	995 $\mu$ l	–	–	3.5 $\mu$ l	1.5 $\mu$ l

CUR: Curcumin; DOX: Doxorubicin; Eth<sup>PEI</sup>: Polyethylenimine-modified ethosome; Eth<sup>SC</sup>: Sodium cholate-modified ethosome.

Table 2. The *in vivo* tested groups and their additives.

	Control	CUR@Eth <sup>PEI</sup>	DOX@Eth <sup>SC</sup>	CUR@Eth <sup>PEI</sup> / DOX@Eth <sup>SC</sup> (7:3)
PBS	300 $\mu$ l	90 $\mu$ l	210 $\mu$ l	–
CUR@Eth <sup>PEI</sup>	–	210 $\mu$ l	–	210 $\mu$ l
DOX@Eth <sup>SC</sup>	–	–	90 $\mu$ l	90 $\mu$ l

CUR: Curcumin; DOX: Doxorubicin; Eth<sup>PEI</sup>: Polyethylenimine-modified ethosome; Eth<sup>SC</sup>: Sodium cholate-modified ethosome; PBS: Phosphate-buffered saline.

### *In vivo* antitumor test of the multidrug-loaded carriers complex

All animal experiments were carried out in accordance with the Institutional Animal Care and Use Committees guidelines. B16 cells ( $1 \times 10^6$ ) were subcutaneously inoculated into the right hind leg of C57BL/6 mice (6–8 weeks, weighting 18–22 g). After 5 days, when the tumor volume of melanoma increased to about 150 mm<sup>3</sup>, the mice were divided randomly into four groups and received transdermal therapy using PBS, CUR@Eth<sup>PEI</sup>, DOX@Eth<sup>SC</sup> and CUR@Eth<sup>PEI</sup>/DOX@Eth<sup>SC</sup>(7:3), respectively (Table 2). For each group, the drugs or PBS were applied to the *in situ* skin of the tumors once every 3 days, totally six-times throughout the experiment. For each time, the *in situ* skin of the tumors (after shaving the hair) were evenly coated with the drugs or PBS and then wrapped with gauze for 24 h. The dose of DOX and CUR was 9 and 21 mg/kg, respectively according to the previous study [17]. The tumor sizes of the mice were measured every 3 days with a caliper in two dimensions. The individual tumor volumes (V) was calculated using the following equation:  $V = (\text{length} \times [\text{width}]^2)/2$ , where length was the longest diameter and width was the shortest diameter [33]. Tumor growth inhibition (TGI) was calculated by the formula:  $\text{TGI} = 1 - (V_{21} - V_0)_{\text{Treatment}} / (V_{21} - V_0)_{\text{Control}}$ , where  $V_{21}$  and  $V_0$  were the individual tumor volumes on day 21 and 0, respectively [33]. Day 0 represents the day when the mice received subcutaneous injection of B16 cells.

### Statistical analysis

All data were reported as mean  $\pm$  standard deviation and the error bars in the figures are the standard deviations of the data. All statistical analysis was used one-way analysis of variance with Origin 8.0 (OriginLab, MA, USA). A p-value of less than 0.05 was considered statistically significant, and a p-value of less than 0.01 was considered highly significant.

## Results

### Physical & chemical properties of the modified ethosomes

ATR-FTIR spectroscopy was used to characterize the changes of the surface chemical compositions of the modified ethosomes. As shown in Figure 1, the characteristic absorption peaks of lecithin mainly include 1743 cm<sup>-1</sup> (C=O stretching vibration), 1158 cm<sup>-1</sup> (C-O antisymmetric stretching vibration), 1080 cm<sup>-1</sup> (C-O-PO<sub>2</sub> characteristic absorption), 988 cm<sup>-1</sup> (RCH = CH<sub>2</sub> characteristic absorption) and 886 cm<sup>-1</sup> (RRC = CHR characteristic absorption) [34]. Cholesterol is characterized by 3400 cm<sup>-1</sup> (OH stretching vibration peak), 2850-2960 cm<sup>-1</sup> (stretching vibration peak of CH<sub>3</sub> bond and stretching vibration joint of CH<sub>2</sub>), 1060 cm<sup>-1</sup> (C-O-(H) stretching vibration) and 1351 cm<sup>-1</sup> (asymmetric deformation vibration joint of CH<sub>3</sub>) [34]. On the spectrum of PEI, 1456 cm<sup>-1</sup> is the bending vibration peak of -NH, 2920 and 2856 cm<sup>-1</sup> are the asymmetric and symmetric stretching vibration peaks of CH<sub>2</sub>, and the strong absorption peak at 3400 cm<sup>-1</sup> is the stretching vibration peak of NH, superimposed with the hydrogen bond vibration peak of water molecules [35]. The bending vibration peak

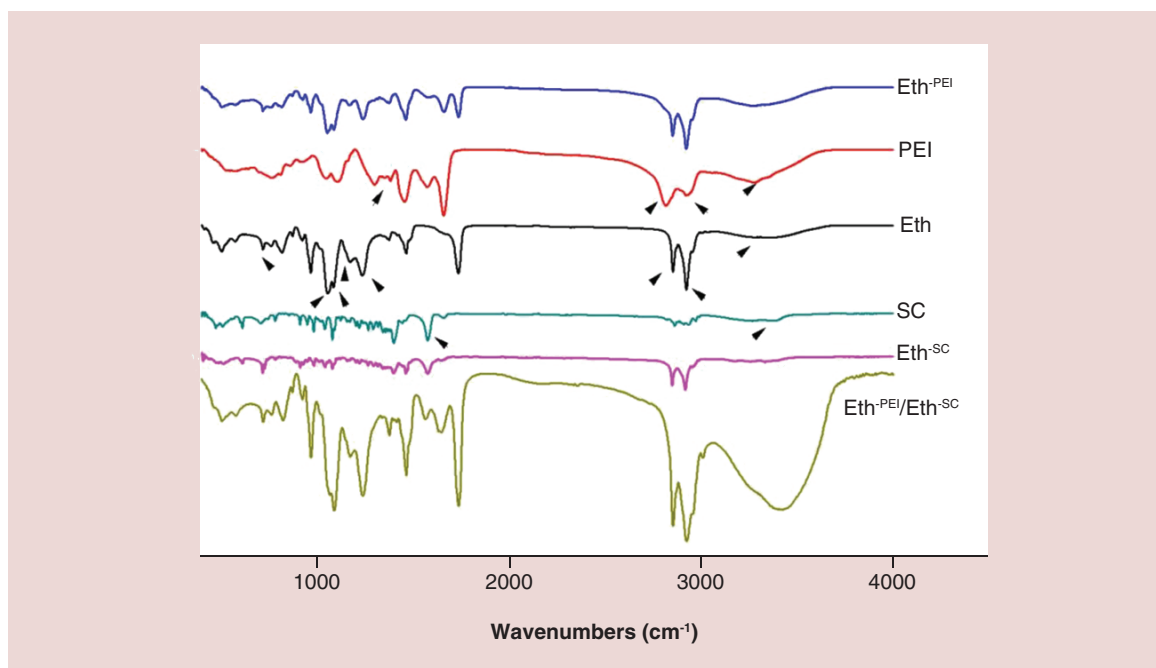


**Figure 1. Attenuated total reflection–Fourier transform infrared spectroscopy spectra of the PEI- or SC-modified ethosomes (the arrows indicate the location of the characteristic peaks).**

Eth<sup>-PEI</sup>: Polyethylenimine-modified ethosome; Eth<sup>-SC</sup>: Sodium cholate-modified ethosome.

of -NH at  $1456\text{ cm}^{-1}$  was not observed in Eth<sup>-PEI</sup> spectrum. While the intensity of other characteristic peaks in Eth<sup>-PEI</sup> was enhanced with the addition of PEI, confirming the successful incorporation of PEI. The characteristic peaks corresponding to the hydroxyl and carbonyl groups were at  $3396$  and  $1676\text{ cm}^{-1}$  respectively on the FTIR spectrum of SC [36]. The intensity of the characteristic peak at  $1676\text{ cm}^{-1}$  in Eth<sup>-SC</sup> was enhanced with the addition of SC, confirming the successful incorporation of SC. Clearly, the main characteristic peaks of PEI, SC and Eth were included in the spectra of Eth<sup>-PEI</sup>/Eth<sup>-SC</sup>.

$\zeta$ -potential was monitored to investigate the surface charge of the modified ethosomes. As shown in Figure 2A, the surface charge of Eth<sup>-PEI</sup> and Eth<sup>-SC</sup> were measured to be  $60.7 \pm 1.5$  and  $-17.6 \pm 0.11$  mV. The charge values of the composite ethosomes were gradually decreased with the amount of Eth<sup>-SC</sup> increased, and Eth<sup>-PEI</sup>/Eth<sup>-SC</sup> (5:5) exhibited a lowest positive charge ( $21.8 \pm 0.15$  mV) (Figure 2A).

The particle size of Eth<sup>-PEI</sup>, Eth<sup>-SC</sup> and the complex was measured by Zetasizer Nano ZS instrument. As shown in Figure 2B, Eth<sup>-PEI</sup> was almost half of the size of Eth<sup>-SC</sup> and the size of the ethosomes complex increased with the proportion of Eth<sup>-SC</sup> increasing, suggesting the aggregation between the two kinds of ethosomes, which was confirmed in the image of TEM (Figure 2C). The morphology of Eth<sup>-PEI</sup>, Eth<sup>-SC</sup> and Eth<sup>-PEI</sup>/Eth<sup>-SC</sup>(7:3) were characterized by TEM (Figure 2C), the carriers have a spherical and multilamellar structure, and the image of Eth<sup>-PEI</sup>/Eth<sup>-SC</sup>(7:3) clearly displayed two or more ethosomes sticking together.

### Cellular uptake of the carriers complex

The RB- or/and FITC-loaded ethosomes (RB@Eth<sup>-PEI</sup>, FITC@Eth<sup>-SC</sup> and RB@Eth<sup>-PEI</sup>/FITC@Eth<sup>-SC</sup>(7:3)) were observed by fluorescence microscopy so as to investigate the cellular uptake of the carriers complex. The RB- or/and FITC-loaded ethosomes were evidently phagocytosed by the B16 cells (Figure 3A). As shown in Figure 3B & C, the fluorescence intensity of the cells ingested the drug-loaded ethosomes was significantly stronger ( $p < 0.01$ ) than that of free drugs (the red fluorescence intensities of RB@Eth<sup>-PEI</sup>, RB@Eth<sup>-PEI</sup>/FITC@Eth<sup>-SC</sup>(7:3) and free RB were  $0.092 \pm 0.01$ ,  $0.095 \pm 0.01$  and  $0.048 \pm 0.005$ , respectively; the green fluorescence intensities of FITC@Eth<sup>-SC</sup>, RB@Eth<sup>-PEI</sup>/FITC@Eth<sup>-SC</sup>(7:3) and free FITC were  $0.052 \pm 0.008$ ,  $0.055 \pm 0.013$  and  $0.028 \pm 0.002$ , respectively), indicating that the carrier-wrapped drugs have a much higher efficiency of cellular uptake than the nude ones do. The intensity values of red or green fluorescence were almost equal for the cells treated with single kind of carriers or the Eth<sup>-PEI</sup>/Eth<sup>-SC</sup>(7:3) (Figure 3B & C) indicating a similar cellular uptake

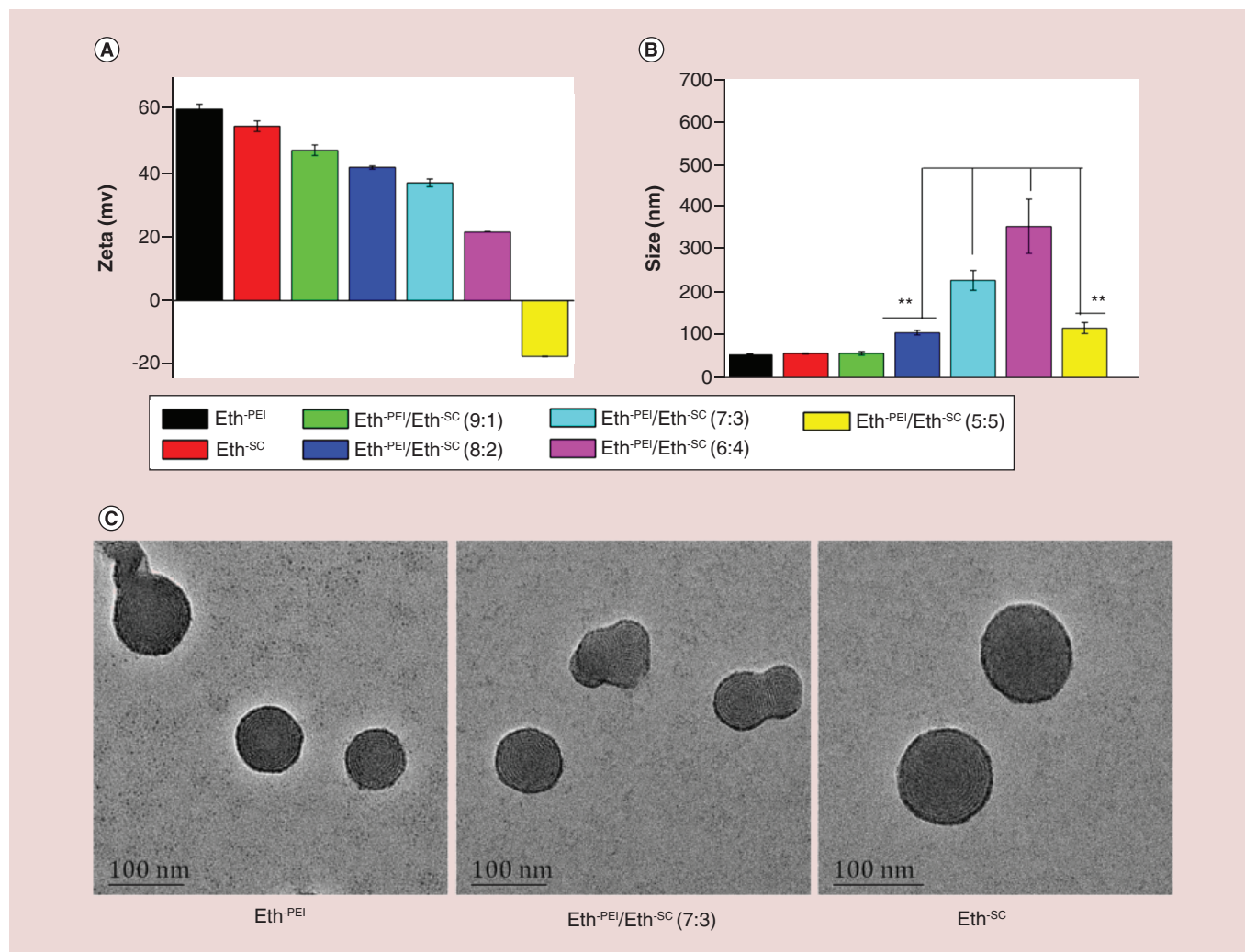


**Figure 2.** Shape, size and surface charge properties of the carrier complex. (A)  $\zeta$ -potential. (B) Particle size. (C) Transmission electron microscopy. \*\* $p < 0.01$ .

Eth<sup>-PEI</sup>: Polyethylenimine-modified ethosome; Eth<sup>-SC</sup>: Sodium cholate-modified ethosome.

rate for single carriers or carriers complex. The results demonstrated the Eth<sup>-PEI</sup>/Eth<sup>-SC</sup>(7:3) has an excellent cellular uptake rate.

### Evaluation of skin permeability of the carriers complex *in vitro*

The transdermal efficiency of the carriers was examined using RB and FITC as the model drugs. As shown in Figure 4A, the fluorescence intensity represents the amount of RB or FITC that penetrated the stratum corneum and remained in the skin tissue. Obviously, the ethosomes-included groups showed much stronger fluorescence intensity than the ones with free drugs (Figure 4A). Moreover, Figure 3B showed RB has a relatively slow release after having experienced the initial burst release at early 20 h. Within 48 h, the cumulative RB release from RB@Eth<sup>-PEI</sup> and RB@Eth<sup>-PEI</sup>/FITC@Eth<sup>-SC</sup>(7:3) rated up to 52.56 and 44.28%, respectively, while that from the group of free RB was only 26.99%. Meanwhile, as shown in Figure 4C, the burst release time of FITC was measured to be 10 h and the cumulative release rates during 48 h of FITC@Eth<sup>-SC</sup> and RB@Eth<sup>-PEI</sup>/FITC@Eth<sup>-SC</sup>(7:3) were 57.71 and 52.16%, respectively, significantly higher than that of the control group with free FITC (38.97%). These results indicated that the Eth<sup>-PEI</sup>/Eth<sup>-SC</sup>(7:3) is effective to transdermally deliver drugs, though its efficiency is slightly less than that of the single ethosomes (Figure 4B & C).

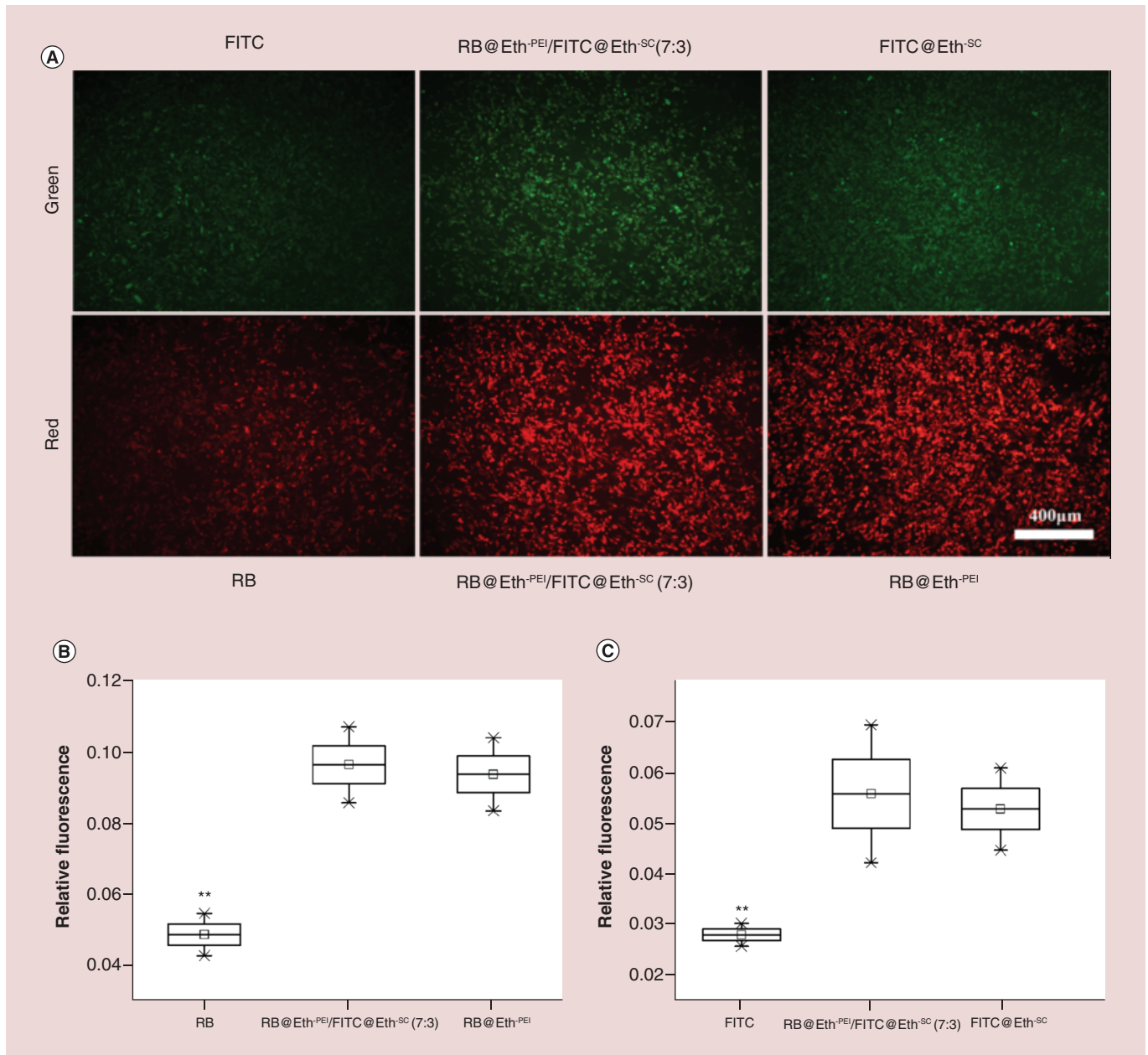


**Figure 3.** The uptake of the carrier complex by B16 cells. (A) Fluorescence images. (b) Fluorescence intensity of RB. (C) Fluorescence intensity of FITC.

\*\* $p < 0.01$ , compared with the other two groups.

Eth<sup>PEI</sup>: Polyethyleneimine-modified ethosome; Eth<sup>SC</sup>: Sodium cholate-modified ethosome; FITC: Fluorescein isothiocyanate; RB: Rhodamine B.

### *In vitro* antitumor effect of the multidrug-loaded carrier complex

Cell viability assay was conducted to evaluate the anticancer activity of the samples *in vitro*. As shown in Figure 5, the viability of B16 cells treated with Eth<sup>PEI</sup> (60 μg/ml) was decreased by 9.65% with the treating time from 12 to 24 h, while little changes appeared for the cells treated with Eth<sup>SC</sup> and Eth<sup>PEI</sup>/Eth<sup>SC</sup>(7:3). The viability test against mouse skin cells L929 also indicated that even at the concentration of 120 μg/ml, both the Eth<sup>SC</sup> and Eth<sup>PEI</sup>/Eth<sup>SC</sup> have good cytocompatibility, better than Eth<sup>PEI</sup> (Supplementary Figure 1). Obviously, the cytotoxicity of Eth<sup>PEI</sup> was significantly reduced by the combination of Eth<sup>SC</sup>. The growth of B16 cells was severely

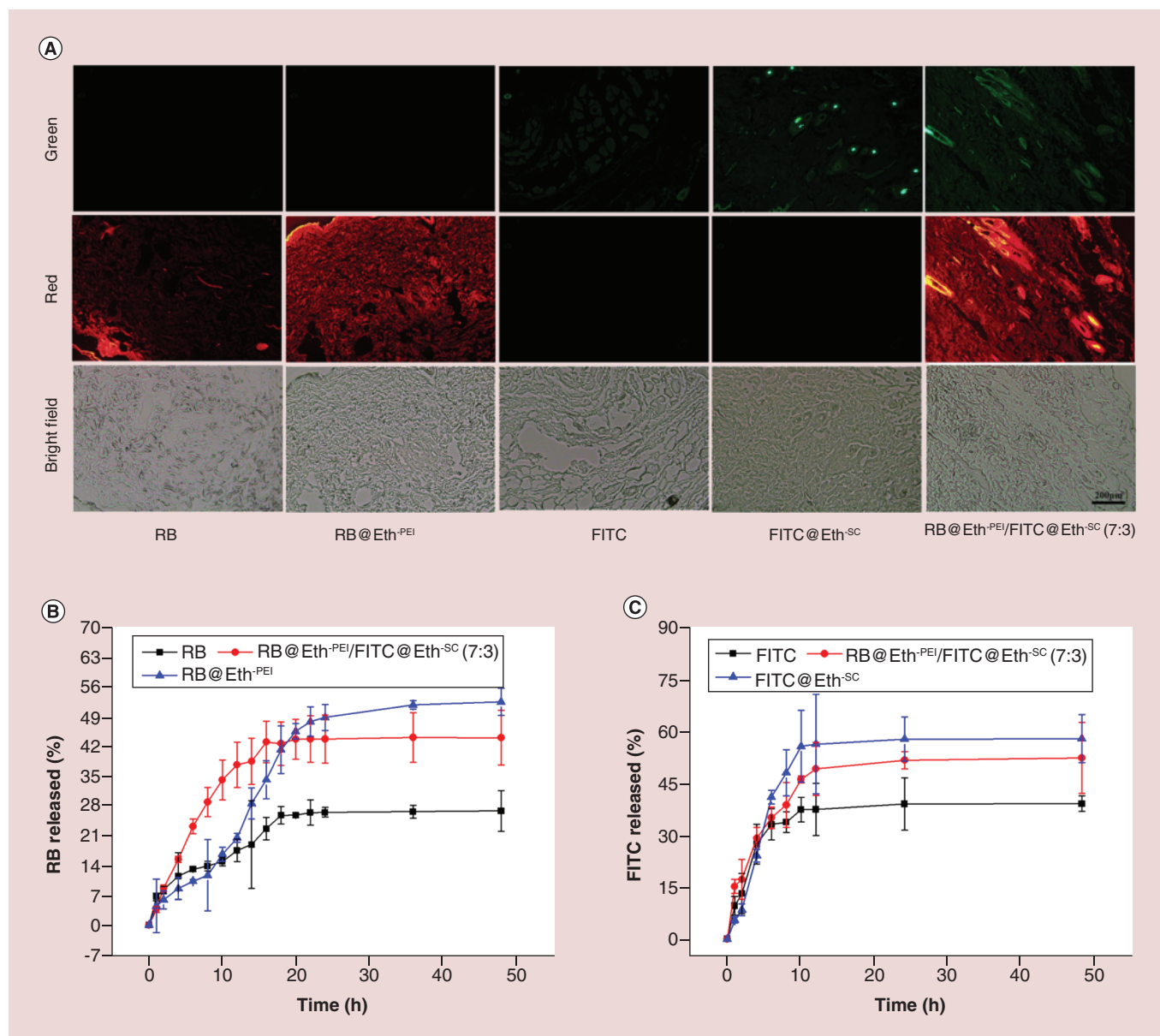


**Figure 4.** Transdermal delivery effect of the carrier complex loading rhodamine B and/or fluorescein isothiocyanate. (A) Distribution of RB or FITC in the skin. (B) Release curve of RB through rat skin. (C) Release curve of FITC through the skin. Eth<sup>PEI</sup>: Polyethylenimine-modified ethosome; Eth<sup>SC</sup>: Sodium cholate-modified ethosome; FITC: Fluorescein isothiocyanate; RB: Rhodamine B.

inhibited by the carriers loading DOX and/or CUR, and among them, the CUR@Eth<sup>PEI</sup>/DOX@Eth<sup>SC</sup>(7:3) exhibited a much stronger inhibition than the CUR@Eth<sup>PEI</sup> or DOX@Eth<sup>SC</sup> did (Figure 5).

#### *In vivo* antitumor efficacy of the multidrug-loaded carrier complex

To further investigate the antitumor efficacy of the drug-loaded carriers via the transdermal route, the C57BL/6 mice bearing melanoma tumor were used (Figure 6A). At the end of the test, all mice were sacrificed and the tumor tissue was excised and photographed. As shown in Figure 6B & C, after the *in situ* transdermal treatment, the tumor volumes of the mice treated with the drug-loaded carriers was significantly smaller than that of the PBS treated ones. From day 5 to 13, the tumor tissue had the fastest growth, during which the tumor volume of the PBS treated mice increased 1065 mm<sup>3</sup>, while that of the mice treated with CUR@Eth<sup>PEI</sup>, DOX@Eth<sup>SC</sup> or CUR@Eth<sup>PEI</sup>/DOX@Eth<sup>SC</sup>(7:3) were 729 mm<sup>3</sup>, 655 mm<sup>3</sup> and 279 mm<sup>3</sup>,

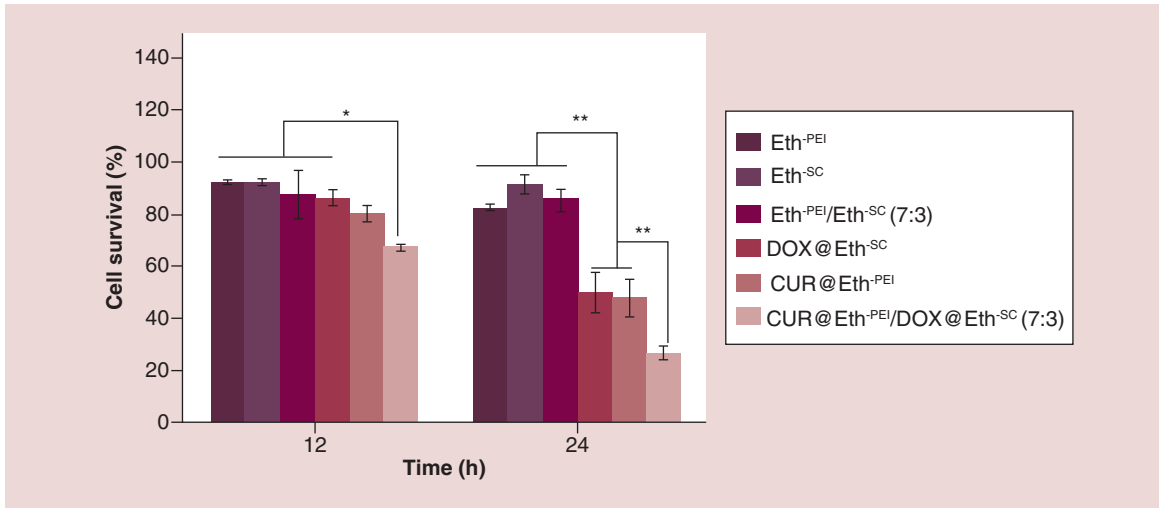


Figure 5. Survival rates of B16 cells treated with different drug-loaded carriers *in vitro*. \*p < 0.05; \*\*p < 0.01.

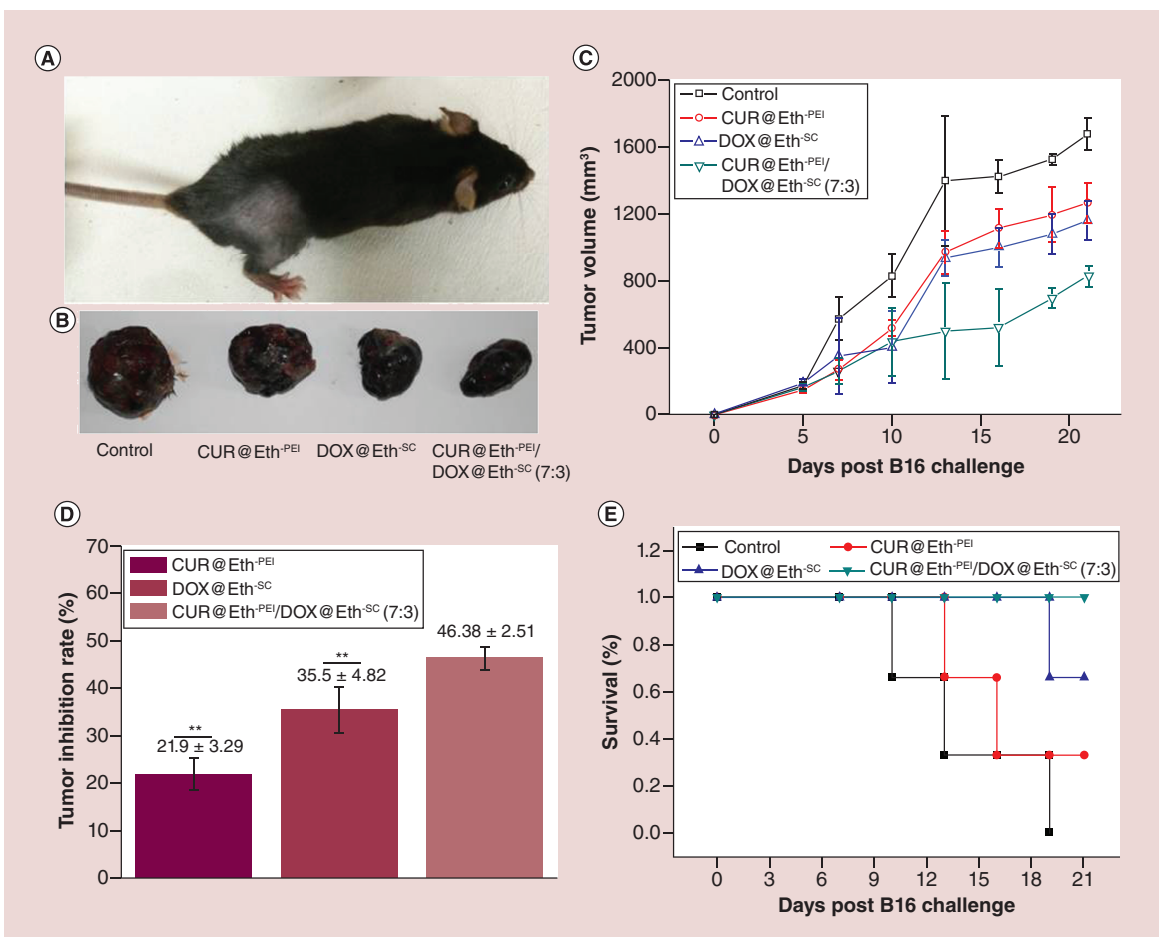


Figure 6. Antitumor effects of drug-loaded carrier complex on melanoma-bearing mice *in vivo*. (A) Melanoma tumor model cured through *in situ* transdermal treatment. (B) The photo images of excised tumor. (C) The growth curves of tumor volume. (D) The rate of tumor inhibition. (E) The survival rates of melanoma-bearing mice treated with different drugs. \*\*p < 0.01, compared with the other two groups.

respectively. As shown in Figure 6D, the tumor inhibition rates were calculated to be 21.9, 35.5 and 46.38% for the mice treated with CUR@Eth<sup>-PEI</sup>, DOX@Eth<sup>-SC</sup> or CUR@Eth<sup>-PEI</sup>/DOX@Eth<sup>-SC</sup>(7:3), respectively. Importantly, the CUR@Eth<sup>-PEI</sup>/DOX@Eth<sup>-SC</sup>(7:3) treated mice showed a much better antitumor ability, compared with those treated by CUR@Eth<sup>-PEI</sup> or DOX@Eth<sup>-SC</sup> ( $p < 0.01$ ). Also, no mice died during the treatment with CUR@Eth<sup>-PEI</sup>/DOX@Eth<sup>-SC</sup>(7:3), while other groups have some deaths (Figure 6E). Obviously, CUR@Eth<sup>-PEI</sup>/DOX@Eth<sup>-SC</sup>(7:3) has excellent antitumor efficacy and significantly prolonged the survival time of the mice bearing melanoma.

## Discussion

The PEI- and SC-modified ethosomes (Eth<sup>-PEI</sup>, Eth<sup>-SC</sup> and Eth<sup>-PEI</sup>/Eth<sup>-SC</sup>) were fabricated and characterized (Figures 1 & 2). As the surface of the cell membrane has a negative charge, carriers with a positive charge on the surface have higher cell transfection ability due to the electrostatic interaction [37]. Thus, the as-prepared carriers complex can be suitable carriers for drug delivery since it possesses a positive charge on the surface. Usually, carriers with small size and more positive charge have better performance on delivering drugs into cells [37]. Although the Eth<sup>-PEI</sup>/Eth<sup>-SC</sup>(9:1) had the smallest size and the most positive charge, the content of Eth<sup>-SC</sup> is too small and would greatly restrict the dose of the loading drug. It was reported that at a low concentration or the concentration difference between the cationic and anionic surfactant is large, not only will there be no obvious aggregation and precipitation, but the certain synergistic effect on promoting the surface activity of materials will occur [38]. While the concentration of the cationic and anionic surfactant is close or the total concentration is high, the mixtures have intrinsic precipitate phenomenon based on strong electrostatic interactions [38], which can explain the aggregation occurred in Eth<sup>-PEI</sup>/Eth<sup>-SC</sup>(6:4) and Eth<sup>-PEI</sup>/Eth<sup>-SC</sup>(5:5) (Supplementary Figure 2). Therefore, the Eth<sup>-PEI</sup>/Eth<sup>-SC</sup>(7:3), with a more positive charge and relatively smaller size, was regarded as the optimal carriers complex for drug delivery.

The uptake rate of tumor cells to drugs is critical for antitumor treatment. Our data showed an excellent uptake of the carriers complex by B16 cells, which is much higher than that of the free drugs. Due to its lipids composition, the ethosomes can cause membrane fusion during the process of endocytosis, which greatly enhances the cellular uptake of the drugs loaded in ethosomes [39,40]. While the uptake of free drugs should be attributed to direct diffusion through cytomembrane, which efficiency is inferior to the ethosome-mediated transportation. Interestingly, the cellular uptake rates were almost no difference between the single carriers and the carriers complex (Figure 2B & C), which indicates that at a certain ratio and concentration, the combination of two carriers does not affect the phagocytosis rates of each one. Our data show a promising potential for the Eth<sup>-PEI</sup>/Eth<sup>-SC</sup>(7:3) serving in drug delivery since it possesses an excellent cellular uptake rate.

Transdermal efficiency is the key parameter of TDDS. As a modified form of liposomes, ethosomes have outstanding transdermal efficiency and stability, making it a competitive candidate using as a drug carrier in TDDS [25]. The high transdermal efficiency of ethosomes should be greatly attributed to the ethanol contained in ethosomes, as the ethanol effectively increases the deformability and mobility of ethosomes [23]. The Franz vertical diffusion method was used to investigate the transdermal performance of the carriers complex, and the temperature of the receiving liquid was set to 37°C according to the previous studies [31,32]. Our data confirms the excellent transdermal performance of the ethosomes (Figure 3). Moreover, the carriers complex of Eth<sup>-PEI</sup>/Eth<sup>-SC</sup>(7:3) also showed a good capacity of penetrating the stratum corneum, indicating the effectiveness of this complex to deliver drugs into the tissues and organs. The transdermal efficiency of Eth<sup>-PEI</sup>/Eth<sup>-SC</sup>(7:3) was slightly less than that of the single ethosomes, which may be due to the larger size of the carriers complex. In consideration of its good performance on both the cellular uptake rate and transdermal efficiency, the complex of Eth<sup>-PEI</sup>/Eth<sup>-SC</sup>(7:3) can be a powerful candidate used as a multidrug carrier in TDDS.

The combination of cytotoxic agent and chemosensitizer, as well as nanocarriers, can help to overcome MDR of cancer [4–6]. Though DOX is an effective cytotoxic agent and widely used in the treatment of cancers, its side effects include MDR, cardiotoxicity and nephrotoxicity, which are almost unavoidable and getting more serious as dose increase [7–9]. In order to reduce DOX dose, CUR can be used as a chemosensitizer. The synergistic effect of CUR and DOX on the treatment of some cancers was reported by several research groups [14–18]. In this study, the combination of DOX and CUR was also adopted to investigate the antimelanoma effect of the as-prepared carriers complex via transdermal route. DOX and CUR were paired with Eth<sup>-SC</sup> and Eth<sup>-PEI</sup>, respectively, owing to the fact that the optimal ratio of Eth<sup>-PEI</sup> to Eth<sup>-SC</sup> for the carriers complex is 7:3 (which means the amount of the drug loaded in Eth<sup>-PEI</sup> would be much larger than the other one loaded in Eth<sup>-SC</sup>) and that DOX has severe side effects

(which greatly restrict its applicative dose) while CUR has no toxic side effects even at high dose. Therefore, it is better to encapsulate CUR into Eth<sup>-PEI</sup>, and DOX into Eth<sup>-SC</sup> so as to obtain a better antitumor effect.

PEI has the ability to efficiently transfect cells due to its large amount of positive charge, but it also has significant cytotoxicity for the same reason. The cytotoxicity of PEI can be reduced with the combination of liposomes according to our previous study (data not shown). Here, our data showed the Eth<sup>-SC</sup> has good cytocompatibility even at a high concentration (600 µg/ml), and the cytotoxicity of Eth<sup>-PEI</sup> was significantly reduced by the combination of Eth<sup>-SC</sup> (Supplementary Figure 1). Melanoma cell line B16 was used to investigate the *in vitro* antitumor ability of the carriers loading DOX and/or CUR. The drug-loaded carriers showed significant cytotoxicity to B16 cells compared with the empty ones. Notably, CUR@Eth<sup>-PEI</sup>/DOX@Eth<sup>-SC</sup>(7:3) exhibited a much better effect on inhibiting the growth of B16 cells compared with CUR@Eth<sup>-PEI</sup> or DOX@Eth<sup>-SC</sup>, which suggested a synergistic effect on anticancer between the CUR@Eth<sup>-PEI</sup> and DOX@Eth<sup>-SC</sup>. Furthermore, the *in vivo* antitumor efficacy of the drug-loaded carriers was evaluated through measuring the tumor sizes of the mice, which showed a similar trend as that of *in vitro* (Figure 6). Both the *in vitro* and *in vivo* data demonstrated the excellent performance of CUR@Eth<sup>-PEI</sup>/DOX@Eth<sup>-SC</sup>(7:3) on inhibiting the growth of the melanoma cells. A synergistic effect of anticancer between CUR@Eth<sup>-PEI</sup> and DOX@Eth<sup>-SC</sup> was also confirmed. Our study indicates that the TDDS based on Eth<sup>-PEI</sup>/Eth<sup>-SC</sup>(7:3) is an effective system loading multidrugs to treat cancer or prevent cancer recurrence after surgery via the transdermal route, especially for the cancers occurred in the skin and subcutaneous tissues.

### Limitations

This study had some limitations. The *in vivo* antitumor efficacy of CUR@Eth<sup>-PEI</sup>/DOX@Eth<sup>-SC</sup>(7:3) has been confirmed through measuring the tumor sizes of the mice and counting the dead individuals. However, it can be better to simultaneously measure the body weight changes of the tested mice. In addition, histological analysis is absent in this work. The histological analysis of the tumor tissue can investigate the infiltration of active T lymphocyte cells, which helps to reveal the antitumor mechanism of the multidrug-loaded carriers complex. In the future, we intend to conduct a more in-depth study of the mechanism of this novel TDDS, and the histological analysis and molecular biological assays will be included. In addition, the final dosage form in this study was a solution which can be inconvenient to use. As a next step, we plan to develop TDDS as easy to use based on the ethosomes complex of this work, constructing a dosage form of nanofibrous mats or hydrogels.

### Conclusion

In this work, a novel TDDS based on Eth<sup>-PEI</sup>/Eth<sup>-SC</sup> complex was successfully produced by electrostatic interaction. The optimal ratio of Eth<sup>-PEI</sup> to Eth<sup>-SC</sup> is 7:3 (in this ratio the output had a higher positive charge and smaller particle size). Moreover, the Eth<sup>-PEI</sup>/Eth<sup>-SC</sup>(7:3) showed good transdermal performance as demonstrated by the experiment *in vitro* using model drugs (RB and FITC). Meanwhile, CUR@Eth<sup>-PEI</sup>/DOX@Eth<sup>-SC</sup>(7:3) showed excellent antitumor activity on the treatment of melanoma *in vitro* and *in vivo*, suggesting this complex a promising potential in transdermally delivering multi drugs to cure cancers occurred in the skin and subcutaneous tissues.

### Future perspective

TDDS has a promising prospect for its outstanding advantages, such as avoiding the first-pass effect of liver and gastrointestinal tract damage to drugs, reducing side effects and improving patient tolerance [26,27]. By enhancing the efficiency of drug administration to the lymphatic system, TDDS has found its unique advantage in the treatment of cancers [28]. The present study reported a new TDDS based on the complex of Eth<sup>-PEI</sup>/Eth<sup>-SC</sup> which can be used as carriers loading cytotoxic agent and chemosensitizer against tumors. We have provided an application example of this TDDS loading DOX and CUR, which showed an excellent performance in the treatment of melanoma. In the next few years, we will improve the Eth<sup>-PEI</sup>/Eth<sup>-SC</sup> based TDDS, such as modifying the surface of the carriers with some tumor-targeting groups, attaching the carriers complex onto a nanofibrous membrane or hydrogel matrix to facilitate its application. As tumor resistance and TDDS continue to be focused, more similar systems with capabilities of multidrug loading and targeted delivery will be developed in the future. For example, some novel tumor immunotherapy system based on TDDS-targeting antigen presenting cells (such as dendritic cells) can be a good choice.

## Summary Points

- A transdermal drug delivery system based on the polyethylenimine (PEI)- and sodium cholate (SC)-modified ethosomes complex (Eth<sup>PEI</sup>/Eth<sup>SC</sup>) has been generated via electrostatic interaction.
- The optimal ratio of Eth<sup>PEI</sup> to Eth<sup>SC</sup> is 7:3, in this ratio the carriers complex (Eth<sup>PEI</sup>/Eth<sup>SC</sup> [7:3]) has a higher positive charge and smaller particle size.
- Eth<sup>PEI</sup>/Eth<sup>SC</sup>(7:3) has a good cellular uptake rate, showing a promising potential in drug delivery.
- Eth<sup>PEI</sup>/Eth<sup>SC</sup>(7:3) showed excellent performance in transdermal drug delivery.
- CUR@Eth<sup>PEI</sup>/DOX@Eth<sup>SC</sup>(7:3) significantly inhibited the growth of melanoma cells *in vitro*.
- CUR@Eth<sup>PEI</sup>/DOX@Eth<sup>SC</sup>(7:3) showed a good effect of inhibiting melanoma *in vivo* through *in situ* transdermal treatment.
- Eth<sup>PEI</sup>/Eth<sup>SC</sup>(7:3) is a useful carrier complex for transdermally deliver multi drugs to cure cancers occurred in the skin and subcutaneous tissues.

## Supplementary data

To view the supplementary data that accompany this paper please visit the journal website at: [www.futuremedicine.com/doi/full/10.2217/nnm-2018-0398](http://www.futuremedicine.com/doi/full/10.2217/nnm-2018-0398)

## Financial &amp; competing interests disclosure

This research was supported by The National Key Research and Development Program of China (2018YFC1706200, 2018YFB1105602), Shanghai Science and Technology Committee Project (18490740400, 17JC1404300), National Natural Science Fund of China (81522049, 31571735, 31270007), Zhejiang Provincial Ten Thousands Program for Leading Talents of Science and Technology Innovation, Zhejiang Provincial Program for the Cultivation of High-level Innovative Health Talents, the “Dawn” Program of Shanghai Education Commission (16SG38), Opening project of Zhejiang provincial preponderant and characteristic subject of Key University, Zhejiang Chinese Medical University (ZYAOX2018035), Project of Health and Family Planning Commission of Zhejiang province (2018KY831) and the Fundamental Research Funds for the Central Universities (2232019D3-20). The authors have no other relevant affiliations or financial involvement with any organization or entity with a financial interest in or financial conflict with the subject matter or materials discussed in the manuscript apart from those disclosed.

No writing assistance was utilized in the production of this manuscript.

## References

Papers of special note have been highlighted as: • of interest; •• of considerable interest

1. Masood F. Polymeric nanoparticles for targeted drug delivery system for cancer therapy. *Mater. Sci. Eng. C Mater. Biol. Appl.* 60, 569–578 (2016).
2. Lentacker I, Geers B, Demeester J, De Smedt SC, Sanders NN. Design and evaluation of doxorubicin-containing microbubbles for ultrasound-triggered doxorubicin delivery: cytotoxicity and mechanisms involved. *Mol. Ther.* 18(1), 101 (2010).
3. Patil RR, Guhagarkar SA, Devarajan PV. Engineered nanocarriers of doxorubicin: a current update. *Crit. Rev. Ther. Drug Carrier Syst.* 25, 1 (2008).
4. Saraswathy M, Gong S. Different strategies to overcome multidrug resistance in cancer. *Biotechnol. Adv.* 31, 1397–407 (2013).
- **Describes tumor resistance and its possible coping strategies.**
5. Yuan M, Qiu Y, Zhang Y *et al.* Targeted delivery of transferrin and TAT co-modified liposomes encapsulating both paclitaxel and doxorubicin for melanoma. *Drug Deliv.* 23, 1171 (2016).
- **Combination of doxorubicin and paclitaxel for the treatment of melanoma.**
6. Hao H, Zhou HS, McMasters KM. Chemosensitization of tumor cells: inactivation of nuclear factor-kappa B associated with chemosensitivity in melanoma cells after combination treatment with E2F-1 and doxorubicin. *Methods Mol. Biol.* 542, 301 (2009).
7. Wan X, Li J, Xie X, Lu W. PTEN augments doxorubicin-induced apoptosis in PTEN-null Ishikawa cells. *Int. J. Gynecol. Cancer* 17, 808–812 (2010).
8. Kim JH, Lee SC, Ro J *et al.* Jnk signaling pathway-mediated regulation of Stat3 activation is linked to the development of doxorubicin resistance in cancer cell lines. *Biochem. Pharmacol.* 79, 373–380 (2010).
9. Ayla S, Seckin I, Tanriverdi G *et al.* Doxorubicin induced nephrotoxicity: protective effect of nicotinamide. *Int. J. Cell Biol.* 2011, 390238 (2011).

10. Hsiao-Sheng L, Ching-Shiun K, Hung-Chi C *et al.* Curcumin-induced mitotic spindle defect and cell cycle arrest in human bladder cancer cells occurs partly through inhibition of aurora A. *Mol. Pharmacol.* 80, 638–646 (2011).
11. Singh M, Singh N. Curcumin counteracts the proliferative effect of estradiol and induces apoptosis in cervical cancer cells. *Mol. Cell. Biochem.* 347, 1–11 (2011).
12. Shin-Hwar W, Liang-Wen H, Jai-Sing Y *et al.* Curcumin induces apoptosis in human non-small cell lung cancer NCI-H460 cells through ER stress and caspase cascade- and mitochondria-dependent pathways. *Anticancer Res.* 30, 2125 (2010).
13. Xia F, Chun Z, Dong-Bo L *et al.* The clinical applications of curcumin: current state and the future. *Curr. Pharm. Des.* 19, 2011–2031 (2012).
14. Sugata B, Soumen S, Goutam M *et al.* Simultaneous delivery of doxorubicin and curcumin encapsulated in liposomes of PEGylated RGDK-lipopeptide to tumor vasculature. *Biomaterials* 35, 1643–1656 (2014).
- **Investigates the antitumor efficacy of doxorubicin and curcumin encapsulated in liposomes.**
15. Zhao X, Qi C, Li Y *et al.* Doxorubicin and curcumin co-delivery by lipid nanoparticles for enhanced treatment of diethylnitrosamine-induced hepatocellular carcinoma in mice. *Eur. J. Pharm. Biopharm.* 93, 27–36 (2015).
16. Wang J, Ma W, Tu P. Synergistically improved anti-tumor efficacy by co-delivery doxorubicin and curcumin polymeric micelles. *Macromol. Biosci.* 15, 1252–1261 (2015).
17. Ma W, Guo Q, Li Y, Wang X, Wang J, Tu P. Co-assembly of doxorubicin and curcumin targeted micelles for synergistic delivery and improving anti-tumor efficacy. *Eur. J. Pharm. Biopharm.* 112, 209–223 (2017).
18. Ranjita M, Sahoo SK. Cof ormulation of doxorubicin and curcumin in poly(D,L-lactide-co-glycolide) nanoparticles suppresses the development of multidrug resistance in K562 cells. *Mol. Pharm.* 8, 852–866 (2011).
- **Investigates the effect of doxorubicin and curcumin-loaded nanoparticles in suppressing multidrug resistance of tumor.**
19. Tejada-Berges T, Granai CO, Gordinier M *et al.* Caelyx/doxil for the treatment of metastatic ovarian and breast cancer. *Expert Rev. Anticancer Ther.* 2, 143–50 (2002).
20. Lowery A, Onishko H, Hallahan DE *et al.* Tumor-targeted delivery of liposome-encapsulated doxorubicin by use of a peptide that selectively binds to irradiated tumors. *J. Control. Release* 150, 117–124 (2011).
21. Ghannam MM, Gebaly RE, Fadel M. Targeting doxorubicin encapsulated in stealth liposomes to solid tumors by non thermal diode laser. *Lipids Health Dis.* 15, 1–8 (2016).
22. Wo Y, Zhang Z, Zhang Y *et al.* Preparation of ethosomes and deformable liposomes encapsulated with 5-fluorouracil and their investigation of permeability and retention in hypertrophic scar. *J. Nanosci. Nanotechnol.* 11, 7840–7847 (2011).
23. Shen LN, Zhang YT, Wang Q *et al.* Enhanced *in vitro* and *in vivo* skin deposition of apigenin delivered using ethosomes. *Int. J. Pharm.* 460, 280–288 (2014).
24. Knudsen KB, Northeved H, Kumar PE *et al.* *In vivo* toxicity of cationic micelles and liposomes. *Nanomedicine* 11, 467–477 (2015).
25. Elsayed MMA, Abdallah OY, Naggat VF, Khalafallah NM. Deformable liposomes and ethosomes: mechanism of enhanced skin delivery. *Int. J. Pharm.* 322, 60–66 (2006).
26. Prausnitz MR, Robert L. Transdermal drug delivery. *Nat. Biotechnol.* 26, 1261–1268 (2008).
27. Prausnitz MR, Samir M, Robert L. Current status and future potential of transdermal drug delivery. *Nat. Rev. Drug Discov.* 3, 115 (2004).
28. Sabitha M, Sanoj RN, Amrita N *et al.* Curcumin loaded chitin nanogels for skin cancer treatment via the transdermal route. *Nanoscale* 4, 239–250 (2011).
- **Demonstrates the effectiveness and unique advantages of transdermal drug delivery system in the treatment of cancer.**
29. Rakesh R, Anoop KR. Formulation and optimization of nano-sized ethosomes for enhanced transdermal delivery of cromolyn sodium. *J. Pharm. Bioallied Sci.* 4, 333–340 (2012).
30. Jiesi X, Yujie J, Wei X *et al.* Hyaluronic acid-containing ethosomes as a potential carrier for transdermal drug delivery. *Colloids Surf. B Biointerfaces* 172, 323–329 (2018).
31. Tsai MJ, Lu IJ, Fu YS *et al.* Nanocarriers enhance the transdermal bioavailability of resveratrol: *in vitro* and *in vivo* study. *Colloids Surf. B Biointerfaces* 148, 650–656 (2016).
32. Kwon SR, Nam SH, Park CY *et al.* Electrodeless reverse electrodialysis patches as an ionic power source for active transdermal drug delivery. *Adv. Func. Mater.* 1705952, 1–10 (2018).
33. Park BN, Lee SJ, Roh JH *et al.* Radiolabeled anti-adenosine triphosphate synthase monoclonal antibody as a theragnostic agent targeting angiogenesis. *Mol. Imaging* 16, 1–10 (2017).
34. Gupta S, Goswami S, Sinha A. A combined effect of freeze–thaw cycles and polymer concentration on the structure and mechanical properties of transparent PVA gels. *Biomed. Mater.* 7, 015006 (2012).
35. Wang F, Liu P, Nie T, Wei H, Cui Z. Characterization of a polyamine microsphere and its adsorption for protein. *Int. J. Mol. Sci.* 14, 17–29 (2012).

36. Sultan AA, El-Gizawy SA, Osman MA, El Maghraby GM. Self dispersing mixed micelles forming systems for enhanced dissolution and intestinal permeability of hydrochlorothiazide. *Colloids Surf. B Biointerfaces* 149, 206–216 (2017).
37. Almofti MR, Harashima H, Shinohara Y *et al.* Cationic liposome-mediated gene delivery: biophysical study and mechanism of internalization. *Arch. Biochem. Biophys.* 410(2), 246–253 (2003).
38. Huang JB, Zhu Y, Zhu BY, Li RK, Fu HL. Spontaneous vesicle formation in aqueous mixtures of cationic surfactants and partially hydrolyzed polyacrylamide. *J. Colloid Interface Sci.* 236(2), 201–207 (2001).
39. Yang L, Wu L, Wu D *et al.* Mechanism of transdermal permeation promotion of lipophilic drugs by ethosomes. *Int. J. Nanomedicine* 12, 3357–3364 (2017).
40. Ascenso A, Raposo S, Batista C *et al.* Development, characterization, and skin delivery studies of related ultradeformable vesicles: transfersomes, ethosomes, and transethosomes. *Int. J. Nanomedicine* 10, 5837–5851 (2015).